Available online at www.sciencedirect.com

SciVerse ScienceDirect

Ceramics International 39 (2013) S545–S548

CERAMICS INTERNATIONAL

www.elsevier.com/locate/ceramint

Sol–gel synthesis of zinc oxide nanoparticles using *Citrus aurantifolia* extracts

Nurul Ain Samat[a,b,*], Roslan Md Nor[a]

[a]*The Department of Physics, Faculty of Science, University of Malaya, 50603 Kuala Lumpur, Malaysia*

[b]*Department of Mathematics & Science, School of Engineering, Science & Technology, Nilai University College, No.1, Persiaran Universiti, Putra Nilai, 71800, Nilai, Negeri Sembilan, Malaysia*

Available online 16 October 2012

Abstract

The use of plant extract in the synthesis of nanostructured materials can be a cost effective and eco-friendly approach. In this paper we report the biosynthesis of zinc oxide nanoparticles using *Citrus aurantifolia* extracts. Spherical zinc oxide nanoparticles were produced using different concentration of zinc acetate which was used as the zinc source. FESEM imaging showed the formation of nanoparticles in the size range of 50–200 nm. XRD analysis revealed wurtzite hexagonal ZnO with preferential orientation at (1 0 0) reflection plane. The room temperature PL spectroscopy showed little variation for samples deposited with different zinc acetate concentration. Peak due to V_o^+, V_o, hole trapped at V_o^{**}, O_i and hydroxyl groups were observed with slight variation in peak position. The synthesis of zinc oxide nanoparticles using the citrus extracts were found to be comparable to those obtained from conventional reduction methods using hexamethylenetetramine or cetyltrimethylammonium bromide and can be an excellent alternative for the synthesis of ZnO nanoparticles using biomaterials.

Keywords: A. Sol–gel process; D. ZnO; Biosynthesis

1. Introduction

Compared to other 1-D semiconductors, ZnO has received its popularity due to the wide band gap and high exciton binding energy (~3.37 eV and 60 meV). The synthesis methods of diversed zinc oxide nanostructures can broadly be classified as two main categories namely gas phase synthesis and solution phase synthesis. Vapour solid (VS), vapour liquid solid, chemical or physical vapour deposition are commonly used gas phase methods [1–4]. While solution phase techniques are the sol–gel, templates assisted and spray pyrolysis [5–7]. The sol–gel method has gained much interest among researchers as it offers controlled consolidation, shape modulation, patterning of the nanostructures [8] and low processing temperature [9].

Recently, biomaterials have been used to synthesize nanoparticles particularly Ag and Au nanoparticles. *Citrus limon* (lemon) [13], *Ocimum sanctum* (Tulsi) leaf [10] and lemongrass plant extract [12] has been used in the synthesis of silver nanoparticles. Also, *Citrus sinensis* peel has been used as reducing and capping agent for Ag nanoparticle synthesis [14]. Extracts from citrus are rich sources of citric acid and ascorbic acid which are excellent reducing agents [15,16]. In the synthesis of ZnO NPs using *Aloe vera* leaf extract, ZnO NPs with average size 25–40 nm was reported. [11].

In this study, we demonstrate a sol–gel technique using *Citrus aurantifolia* fruit extract to synthesize ZnO nanoparticles. Zinc acetate at different concentrations was used as the zinc source with the pH and synthesis temperature was kept constant. The as-synthesized nanoparticles were then characterized using FESEM, XRD and PL spectroscopy.

2. Materials and methods

C. aurantifolia fruits obtained from the local market were peeled and the pulps were sliced into small pieces and

*Corresponding author at: University of Malaya, The Department of Physics, Faculty of Science, 50603 Kuala Lumpur, Malaysia. Tel.: +379674285; fax: +379674146.

E-mail address: ainsamat@siswa.um.edu.my (N. Ain Samat).

0272-8842/$ - see front matter © 2012 Elsevier Ltd and Techna Group S.r.l. All rights reserved.
http://dx.doi.org/10.1016/j.ceramint.2012.10.132

blended in DI water. The blended pulps were then filtered using muslin cloth to remove solid particles. The liquid was further filtered using syringe filter with a pore size of 200 nm. Zinc acetate was dissolved in 100 mL of the filtered *C. aurantifolia* liquid extracts at concentrations of 0.05 M, 0.10 M, 0.15 M and 0.20 M. The pH value of the solution was between 3.7 and 4.0. The mixtures were heated to 90 °C under continuous stirring for 3 h after which white precipitate occurred. The precipitates were recovered, thoroughly rinsed in DI water and dried at 100 °C for 6 h.

The samples were analyzed using FESEM imaging, XRD analysis using probe at 1.5406 Å and PL spectroscopy using the He–Cd laser beam at 325 nm.

3. Results and discussion

Fig. 1 shows photographs of an example of zinc oxide nanoparticles synthesized. Fig. 1(a) shows solution of precipitated ZnO after reaction and in Fig. 1(b) shows ZnO sample after being heated for 6 h. Fig. 2 shows the FESEM micrographs of ZnO particles synthesized at 90 °C for 3 h at 0.05 M, 0.10 M, 0.15 M, and 0.20 M, respectively. It can be seen from the micrographs that the size of particles decreases with increasing Zn acetate concentration. A non-uniform surface morphology was clearly observable from the lowest concentration (Fig. 2a), revealing no particles formed. When the concentration of Zn in citrus extract was increased to 0.10 M (Fig. 2b), it can be seen that the particles agglomerated at certain places and the diameters of the particles varies approximately between 0.15 μm and 0.35 μm. Fig. 2c and d showed that the particles are homogeneous with good nanostructures. ZnO nanoparticles are mostly in spherical shape. From the SEM images for ZnO synthesized at 0.15 M and 0.20 M looks uniform with structures of about 100 nm. The XRD patterns of ZnO nanostructures are shown in Fig. 3. The XRD pattern at 0.10 M exhibited the XRD pattern similar to 0.15 M and 0.20 M. For all samples, peaks from the (1 0 0) reflection plane dominated with peaks due to the (1 0 1), (1 0 2) and (1 1 0) appear to be subdued. It seemed that the ZnO NPs has preferential orientation at (1 0 0). While the peaks labeled with stars were assigned to $Zn(OH)_2$.

Fig. 4 shows the visible PL spectra for the ZnO NPs synthesized at different Zn acetate concentrations. The overlapping broad peaks were fitted with Gaussian curves. The results are summarized in Table 1. Considering the sample synthesized at 0.05 M zinc acetate concentration, peak at 451.5 nm can be attributed to ionized oxygen vacancy [21,22]. This peak was also present in other samples seemed to be slightly re-shifted with increasing zinc acetate concentration. Peak at about 490 nm was attributed to transition from oxygen vacancy [17] which was also present in all samples but showed a trend of being blue-shifted with increasing zinc acetate concentration. Peak at about 535 nm was attributed to transition from hole trapped at the doubly ionized oxygen vacancy [18]. Lastly PL peak at about 580 nm was due to oxygen

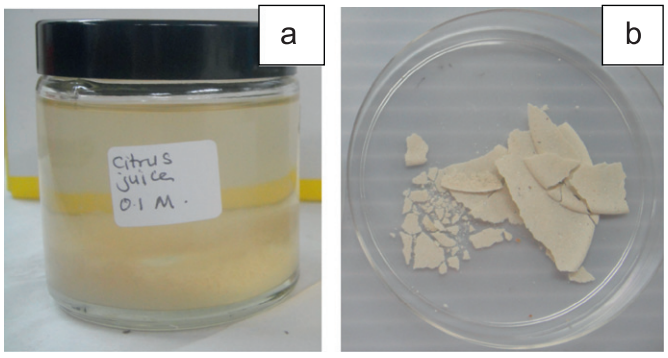

Fig. 1. Photograph of (a) 0.1 M zinc acetate in *C. aurantifolia* extract after being heated for 3 h at 90 °C and (b) the precipitate after being heated at 100 °C for 6 h.

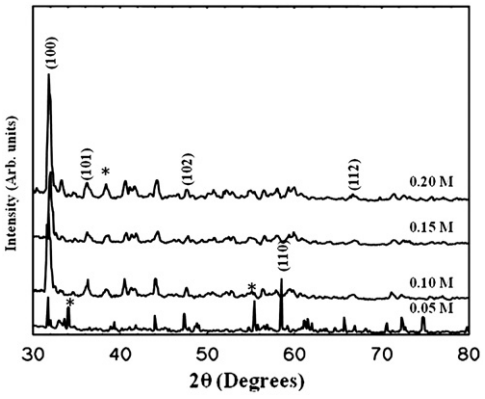

Fig. 3. XRD patterns of ZnO nanostructures synthesized at concentration of (a) 0.05 M, (b) 0.10 M, (c) 0.15 M and (d) 0.2 M. Peaks from $Zn(OH)_2$ are labeled with star.

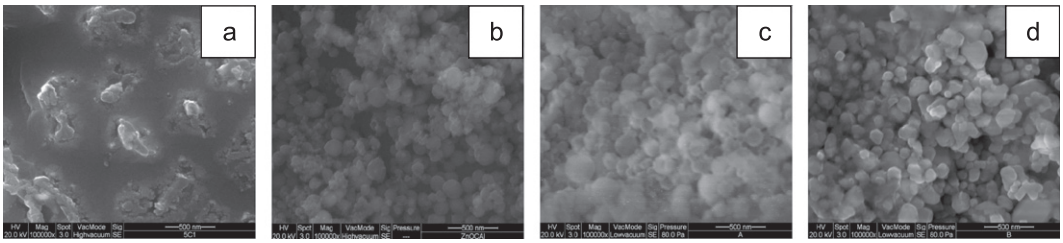

Fig. 2. SEM images of ZnO particles synthesized using Zinc acetate at concentrations of (a) 0.05 M, (b) 0.10 M and (c) 0.15 M (d) 0.20 M.

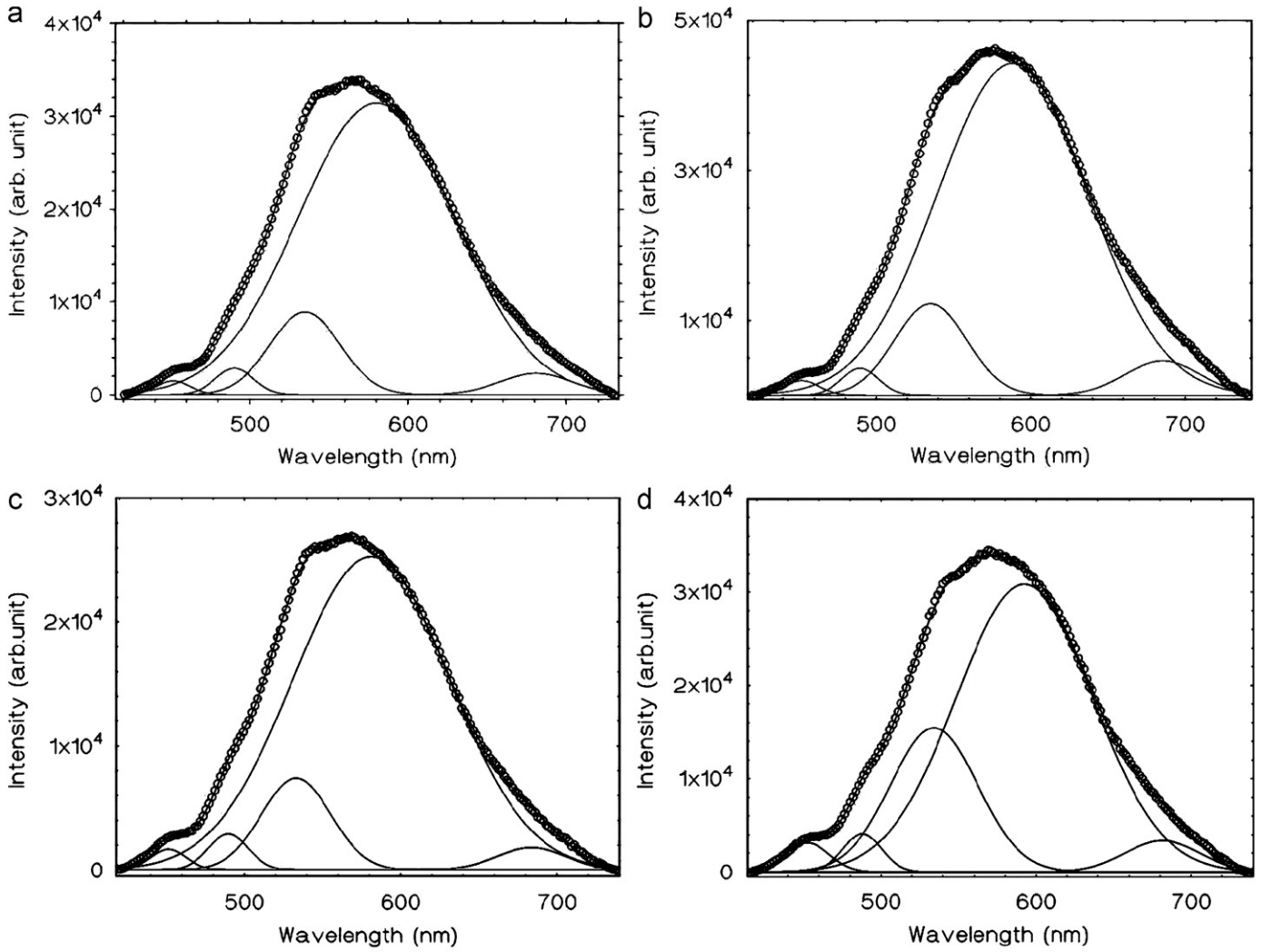

Fig. 4. PL spectra in the yellow green region fitted to Gaussian curves for samples synthesized using Zn acetate dehydrate at concentration of (a) 0.05 M, (b) 0.10 M, (c) 0.15 M and (d) 0.20 M. (For interpretation of the references to color in this figure legend, the reader is referred to the web version of this article.)

Table 1
The PL peaks for ZnO samples synthesized at different zinc acetate concentration.

Zn Acetate concentration	PL peak (nm)	Proposed transition	Refs.
0.05 M	451.484	Ionized oxygen vacancies	21,22
	490.178	Oxygen vacancy	17
	534.837	hole trapped at V_o**	18
	579.979	oxygen interstitials	20
0.10 M	451.693	Ionized oxygen vacancies	21,22
	489.474	Oxygen vacancy	17
	535.176	hole trapped at V_o**	18
	588.357	oxygen interstitials	20
0.15 M	451.422	Ionized oxygen vacancies	21,22
	489.667	Oxygen vacancy	17
	533.125	hole trapped at V_o**	18
	581.249	oxygen interstitials	20
0.20 M	452.374	Ionized oxygen vacancies	21,22
	487.855	Oxygen vacancy	17
	534.147	hole trapped at V_o**	18
	592.496	hydroxyl groups	19

interstitials [20] was present in all samples except at zinc concentration of 0.2 M where a peak attributed to hydroxyl group was observed at 592 nm and it is attributed to structural defect, single ionized vacancy and impurities [22,23]. Broad yellow band has been cited in many studies due to the fact it is commonly observed in sample grown by solution methods. Study reveals this band may be attributed to the presence of hydroxyl groups [19].

4. Conclusions

ZnO NPs have been successfully synthesized in *C. aurantifolia* extract at different Zn acetate concentrations via sol–gel method. XRD analysis showed preferred orientation at the (1 0 0) reflection plane with significantly subdued peaks in the (1 0 1), (1 0 2), (1 1 0) and (1 1 2) planes. Room temperature PL analysis in the visible region showed peaks attributed to the conventional defect states for ZnO. In general, we have demonstrated that *C. aurantifolia* extract is viable for the synthesis of ZnO NPs utilizing the sol–gel technique where such biosynthesis offers an alternative for a green synthesis method.

Acknowledgments

This work was partially supported by Ministry of Higher Education of Malaysia FRGS Grant No: FP050/2008C, University of Malaya PPP Grant No. PV072/2012A and Nilai University College under Grant No. MS 001.

References

[1] C.C. Tang, S.S. Fan, Lamy de la, M. Chapelle, P. Li, Silica-assisted catalytic growth of oxide and nitride nanowires, Chemical Physics Letters 333 (2001) 12.
[2] Z. Wang, H.L. Li, Highly ordered zinc oxide nanotubules synthesized within the anodic aluminum oxide template, Applied Physics A 74 (2002) 201.
[3] L. Miao, Y. Ieda, S. Tanemura, Y.G. Cao, M. Tanemura, Y. Hayashi, S. Toh, K. Kaneko, Synthesis microstructure and photoluminescene of well-aligned ZnO nanorods on Si substrate, Science and Technology of Advanced Materials 8 (2007) 443.
[4] Y. Satoh, S. Ohshio, H. Saitoh, Photoluminescene spectroscopy of highly oriented Y_2O_3:Tb crystalline whiskers, Science and Technology of Advanced Materials 6 (2005) 215.
[5] L. Spanhel, Colloidal ZnO nanostructures and functional coatings: a survey, Journal of Sol–Gel Science and Technology 39 (2006) 7.
[6] S. Shingubara, Fabrication of nanomaterials using porous alumina templates, Journal of Nanoparticle Research 5 (2003) 17.
[7] R. Ayouchi, F. Martin, D. Leinen, J.R. Ramos-Barrado, Growth of pure ZnO thin films prepared by chemical spray pyrolysis on silicon, Journal of Crystal Growth 247 (2003) 497–504.
[8] B. Sunandan, D. Joydeep, Hydrothermal growth of ZnO nanostructures, Science and Technology of Advanced Materials 10 (2009) 013001.
[9] E.G. Lori, D.Y. Benjamin, L. Matt, Z. David, Y. Peidong, Solution-grown zinc oxide nanowires, Inorganic Chemistry 45 (2006) 7535–7543.
[10] G. Singhal, R. Bhavesh, K. Kasariya, A.R. Sharma, R.P. Singh, Biosynthesis of nanoparticles using *Ocimum sanctum* (Tulsi) leaf extract and screening its antimicrobial activity, Journal of Nanoparticle Research 13 (2011) 2981–2988.
[11] G. Sangeetha, S. Rajeshwari, R. Venckatesh, Green synthesis of zinc oxide nanoparticles by *Aloe barbadensis* miller leaf extract: structure and optical properties, Materials Research Bulletin 46 (2011) 2560–2566.
[12] A. Rai, M. Chaudhary, A. Ahmad, S. Bhargava, M. Sastry, Synthesis of triangular Au core–Ag shell nanoparticles, Materials Research Bulletin 42 (2007) 1212.
[13] T.C. Prathna, N. Chandrasekaran, Ashok M. Raichur, Amitava Mukherjee, Biomimetic synthesis of silver nanoparticles by *Citrus limon* (lemon) aqueous extract and theoretical prediction of particle size, Colloids Surfaces B 82 (2011) 152–159.
[14] S. Kaviya, J. Santhanalakshmi, B. Viswanathan, J. Muthumary, K. Srinivasan, Biosynthesis of silver nanoparticles using *Citrus sinensis* peel extract and its antibacterial activity, Spectrochimica Acta Part A: Molecular and Biomolecular 79 (2011) 594–598.
[15] O.B. Garcia, J. Castillo, J.R. Marin, A. Ortuno, J.A. Del Rio, Uses and properties of citrus flavonoids, Journal of Agriculture and Food Chemistry 45 (1997) 4505–4515.
[16] J.A. Vinson, X. Su, L. Zubik, P. Bose, Phenol antioxidant quantity and quality in foods: fruits, Journal of Agriculture and Food Chemistry 49 (2001) 5315–5321.
[17] M.K. Patra, K. Manzoor, M. Manoth, S.P. Vadera, N. Kumar, Journal of Luminescence 128 (2) (2008) 267–272.
[18] A. van Dijken, E.A. Meulenkamp, D. Vanmaekelbergh, A. Meijerink, Enhancement of ZnO photoluminescene by localized and propagating surface plasmons, Journal of Physical Chemistry B 104 (8) (2000) 1715–1723.
[19] K.H. Tam, C.K. Cheung, Y.H. Leung, A.B. Djuřišić, C.C. Ling, C.D. Beling, S. Fung, W.M. Kwok, W.K. Chan, D.L. Phillips, L. Ding, W.K. Ge, Defects in ZnO nanorods prepared by a hydrothermal method, Journal of Physical Chemistry B110 (42) (2006) 20865–20871.
[20] D. Li, Y.H. Leung, A.B. Djurišić, Z.T. Liu, M.H. Xie, S.L. Shi, S.J. Xu, W.K. Chan, Different origins of visible luminescene in ZnO nanostructures fabricated by the chemical and evaporation methods, Applied Physics Letters 85 (9) (2004) 1601–1603.
[21] C.L. Xu, D.H. Qin, H. Li, Y. Guo, T. Xu, H.L. Li, Low temperature growth and optical properties of radial ZnO nanowires, Materials Letters 58 (2004) 3976–3979.
[22] K. Vanheusden, W.L. Warren, C.H. Seager, D.R. Tallant, J.A. Voigt, B.E. Gnade, Mechanisms behind green photoluminescence in ZnO phosphor powders, Journal Applied Physics 79 (1996) 7983–7990.
[23] J.J. Wu, S.C. Liu, Low-Temperature growth of well-aligned ZnO nanorods by chemical vapor deposition, Advanced Materials 14 (2002) 215–218.